A Numerical Model for Water Flow and Chemical Transport in Variably Saturated Porous Media

by T.-C. Jim Yeh, Rajesh Srivastava, Amado Guzman, and Thomas Harter[a]

Abstract

A two-dimensional numerical model is developed for the simulation of water flow and chemical transport through variably saturated porous media. The nonlinear flow equation is solved using the Galerkin finite-element technique with either the Picard or the Newton iteration scheme. A continuous velocity field is obtained by separate application of the Galerkin technique to the Darcy's equation. A two-site adsorption-desorption model with a first-order loss term is used to describe the chemical behavior of the reactive solute. The advective part of the transport equation is solved with one-step backward particle tracking while the dispersive part is solved by the regular Galerkin finite-element technique. A preconditioned conjugate gradient-like method is used for the iterative solution of the systems of linear simultaneous equations to save on computer memory and execution time. The model is applied to a few flow and transport problems, and the numerical results are compared with observed and analytic values. The model is found to duplicate the analytic and observed values quite well, even near very sharp fronts.

Introduction

Until the early 1970s, studies of flow and transport through unsaturated soils were limited to the upper one meter of the vadose zone and were done primarily with agricultural purposes in mind. In the last 20 years, because of the important role of the vadose zone in ground-water pollution problems, hydrologists have become increasingly interested in studies involving unsaturated flow and transport problems on scales of meters and tens of meters. At such large scales, the hydrological properties of the geologic media exhibit a large degree of spatial variation. For investigating and predicting contaminant migration in large-scale geologic media, mathematical modeling is generally required. Moreover, analytic solutions to such problems are almost impossible to obtain, and numerical modeling becomes the method of choice for analyzing and predicting the movement of contaminants through the subsurface media (Anderson, 1979). The mathematical models are generally based on the governing equation of flow under variably saturated conditions (Richards' equation) and the classic convection-dispersion equation. One of the difficulties in predicting the movement of contaminants lies in our lack of ability to solve these equations accurately and efficiently for general cases.

The dependence of hydraulic properties of unsaturated media on the pressure or degree of saturation makes the Richards equation nonlinear. The degree of nonlinearity of the equation, in turn, depends on the extent of the nonlinearity in hydraulic properties and pressure relationships of media. In general, numerical methods combined with some iterative schemes are required to obtain the solution to this equation. Since hydraulic properties and pressure relationships of some porous media are highly nonlinear, difficulties in obtaining the convergence of the numerical solution and serious mass balance problems have often been encountered (e.g., Celia et al., 1990).

The solution of the convection-dispersion equation requires the knowledge of the velocity distribution throughout the solution domain. Many difficulties exist in calculating the velocity field from the pressure distribution obtained by numerical models. As is customary for finite-element flow simulations, the nodal heads are treated as unknowns and assumed to vary linearly in triangular elements and bilinearly in rectangular elements. This results in a constant specific discharge value within each element and consequently in a discontinuity in the nodal values of the specific discharge. Such a discontinuous discharge field may lead to undesirable numerical solutions of the convection-dispersion equation (e.g., Goode, 1990). Although the mixed finite-element approach (e.g., Chiang et al., 1989) can alleviate this problem, it produces a large system of equations to be solved and thus increases the computational effort. In addition, for highly heterogeneous aquifers, the matrix equations are in general poorly conditioned (Allen et al., 1992).

Another difficulty in solving the convection-dispersion equation can be attributed to the change in the nature of the equation from parabolic to almost hyperbolic as the advective transport becomes prominent relative to the dispersive transport (manifested by a large Peclet number). While a parabolic partial differential equation is amenable to the commonly used numerical methods like finite difference or finite elements, numerical solution to a hyperbolic equation by these methods generally introduces numerical dispersion

[a]Associate Professor, and Graduate Students, respectively, Department of Hydrology and Water Resources, The University of Arizona, Tucson, Arizona 85721.

Received July 1992, revised January 1993, accepted February 1993.

or oscillation near the sharp front. This problem can be tackled, to some extent, by a properly chosen grid size and time step at the expense of increased computer time and memory requirements (Daus et al., 1985). Various alternative approaches have been suggested in the past to reduce the numerical error near the sharp fronts. These include the implicit diffusive finite-difference method (Yanosik and McCracken, 1979), upstream weighted finite-element method (Huyakorn and Nilkuha, 1979), method of characteristics (Konikow and Bredehoeft, 1978), modified method of characteristics (Chiang et al., 1989), Laplace transform-Galerkin technique (Sudicky, 1989), and the zoomable hidden mesh approach (Yeh, 1990). The method of characteristics (also called forward particle tracking) and the modified method of characteristics (backward particle tracking) have been combined successfully by some investigators (Neuman, 1984; and Cady, 1991). This scheme has been shown to handle the sharp fronts very well but is computationally intensive.

Most of the schemes described above perform well under saturated flow conditions, but have not been rigorously tested for unsaturated conditions. Also, there are very few numerical codes for simulation of two-dimensional flow and transport of reactive chemicals in variably saturated media. In this paper, we combine several previously developed ideas and construct an efficient, two-dimensional finite-element model, which alleviates the difficulties discussed above. The model was applied to several scenarios where either analytical or observed data are available for verification purposes. In addition, analytical solutions of the velocity field in a two-dimensional unsaturated medium with exponential hydraulic properties were derived and used to verify the accuracy of the numerical model. We believe the model will enhance our ability of predicting flow and fate and transport of contaminants in the field, where hydraulic and geochemical properties of the media are inherently heterogeneous.

Governing Equations

Equation of Flow in Variably Saturated Media

The following equation is taken as the equation governing two-dimensional flow of water in porous media (Bear, 1979)

$$\frac{\partial}{\partial x_i}\left(K_{ij}\frac{\partial}{\partial x_j}(\psi+\beta_g x_2)\right)= (C+\beta_s S_s)\frac{\partial \psi}{\partial t} - q_s \qquad \text{in } \Omega \qquad (1)$$

where x_i and x_j are the spatial coordinates ($i, j = 1, 2$) with x_2 being the vertical upward direction for vertical flow; K_{ij} is the hydraulic conductivity tensor which under unsaturated conditions is a function of moisture content or pressure; ψ is the pressure head; C is the specific moisture capacity defined as $d\theta/d\psi$ where θ is the volumetric moisture content; β_g is the index for gravity and is zero for horizontal flow and one for vertical flow; β_s is the index for saturation and is zero in the unsaturated zone ($\psi < 0$) and one in the saturated zone ($\psi \geq 0$); S_s is the specific storage defined as the volume of water released from storage per unit volume of saturated soil due to a unit decrease in the pressure head; t is the time; q_s is the source/sink term (positive for source) which represents the volume of water added/removed per unit time to/from a unit volume of soil; and Ω is the solution domain. Einstein's summation convention (over repeated index) has been used in the above equation and throughout this paper.

Equations for Transport and Fate of Contaminants

The complex process of dispersion, adsorption, and decay of chemicals in porous media flow is not very well understood at the present time, and various models have been proposed to describe the interaction between solute, pore water, and the solid matrix in a porous medium. These models include a simple linear isotherm equilibrium model (Rubin, 1983), a linear reversible adsorption (one-site) model (Lindstrom and Boersma, 1973), a two-site adsorption-desorption model (Selim et al., 1976; Cameron and Klute, 1977), mobile-immobile zone physical partitioning model (Deans, 1963; Coats and Smith, 1964; van Genuchten and Wierenga, 1976), mobile-immobile zone with ion exchange (Krupp et al., 1972), and the two-site model with a first-order loss (Lassey, 1988). It has been shown (Nkedi-Kizza et al., 1984) that although the physical partitioning model with mobile and immobile zones and the two-site chemical partitioning model are completely different concepts, they result in the same mathematical equation. Also, Lassey's (1988) model is quite general and encompasses, as special cases, the physical and chemical partitioning models. In this paper, therefore, the two-site model with first-order loss was used to represent the complex process of chemical transformation of the solute.

By using the formulation of Cameron and Klute (1977) and adding a first-order loss term (Lassey, 1988), the equation governing the transport of a chemically reactive solute is

$$\frac{\partial}{\partial x_i}\left(D_{ij}\frac{\partial c}{\partial x_j}\right) - q_i\frac{\partial c}{\partial x_i} = \theta\frac{\partial c}{\partial t} + \frac{\partial(\rho_b c^*)}{\partial t} + f k_2 \rho_b c_k^* + q_s(c - c_s) \qquad \text{in } \Omega \qquad (2a)$$

With

$$\frac{\partial(\rho_b c^*)}{\partial t} = k_1\theta c - k_2\rho_b c_k^* + \frac{\partial(\rho_b c_e^*)}{\partial t} \qquad (2b)$$

where c is the solute concentration in the liquid (in units of mass per unit volume); c^* is the adsorbed phase concentration (in units of mass of adsorbed chemical per unit mass of porous media); c_k^* is the kinetic fraction of the adsorbed chemical, and c_e^* ($= k_3\theta c/\rho_b$) is the equilibrium fraction; k_1 is the forward (adsorption) rate constant, k_2 is the backward (desorption) rate constant, and k_3 is the equilibrium constant; f is the loss coefficient for the selective first-order removal; q_i are the specific discharge components; ρ_b is the bulk density; q_s is the injected/pumped fluid volume per unit aquifer volume; and c_s is the solute concentration in q_s. D_{ij} is the hydrodynamic dispersion tensor computed on the basis of the specific discharge and is given by:

$$D_{ij} = (\alpha_L - \alpha_T)\frac{q_i q_j}{q} + \alpha_T q \delta_{ij} + D_0 \qquad (2c)$$

in which α_L is the longitudinal dispersivity; α_T is the transverse dispersivity; $q = (q_i q_i)^{1/2}$ and is the magnitude of the specific discharge; δ_{ij} is the Kronecker delta ($\delta_{ij} = 1$, if $i = j$ and 0 otherwise); and D_0 is the apparent molecular diffusion.

Numerical Scheme

Equation (1) is solved using the Galerkin technique by representing the pressure at any point (x_1, x_2) in the domain at any instant t as:

$$\psi(x_1, x_2, t) = N_I(x_1, x_2)\,\psi^I(t) \qquad (3)$$

where N_I are the shape functions associated with node I; and ψ^I is the value of ψ at node I with the range of I being from 1 to NN (NN is the total number of nodes). Linear shape functions for triangular elements and bilinear shape functions for the rectangular and quadrilateral elements are used in this study. In a similar way the hydraulic conductivity tensor and the moisture capacity term are represented as

$$[K] = N_I[K]^I \qquad (4a)$$

and

$$C = N_I C^I \qquad (4b)$$

where [K] and C are the conductivity tensor and the moisture capacity at any point in the domain at any time, and $[K]^I$ and C^I are the nodal values. Strictly speaking, equations (4a) and (4b) are inconsistent with equation (3) because of the nonlinear relations between the pressure head and the unsaturated hydraulic conductivity, and relations between the pressure head and the moisture capacity term. Errors due to this inconsistent approach may, however, be resolved by using small elements. After these values of ψ, K, and C are put in equation (1), a residual R_ψ is obtained as

$$R_\psi = \frac{\partial}{\partial x_i}\left(N_L K_{ij}^L \frac{\partial}{\partial x_j}(N_J \psi^I + \beta_g x_2)\right) - (N_L C^L + \beta_s S_s)\frac{\partial (N_J \psi^I)}{\partial t} - q_s \qquad (5)$$

Now, using the Galerkin scheme, NN equations are obtained as follows:

$$\int_\Omega R_\psi N_I \, d\Omega = 0 \qquad \text{for } I = 1 \text{ to NN} \qquad (6)$$

These equations can be more conveniently and concisely written in the matrix form, after making use of the divergence theorem and noting that the shape function for any node is nonzero only in elements containing that node, as:

$$[A]\{\psi\} + [B]\frac{\partial}{\partial t}\{\psi\} + \{F\} - \{Q\} = 0 \qquad (7)$$

where $\{\psi\}$ is the vector of the nodal values of the pressure head; [A] is the conductance matrix; [B] is the storage matrix; {F} is the gravity vector; and {Q} is the flux vector. These matrices and vectors are given by the following equations:

$$A_{IJ} = \Sigma_e \int_{A^e} \frac{\partial N_I}{\partial x_i}\left(N_L K_{ij}^L \frac{\partial N_J}{\partial x_j}\right) dA \qquad (8a)$$

$$B_{IJ} = \Sigma_e \int_{A^e} (N_L C^L + \beta_s S_s) N_I N_J \, dA \qquad (8b)$$

$$F_I = \Sigma_e \int_{A^e} \frac{\partial N_I}{\partial x_i}(N_L K_{i2}^L)\, dA \qquad (8c)$$

$$Q_I = \Sigma_e \left(\int_{A^e} - N_I q_s \, dA + \int_{B^e} N_I q_b \, dB\right) \qquad (8d)$$

in which the integrals are performed over all elements containing node I as one of their nodes, and the boundary integral in equation (8d) is evaluated along the boundaries of elements which lie along the boundary of the domain with specified normal flux q_b. A^e represents the area of the element and B^e its boundary. It should be noted that the storage matrix B as given by equation (8b) is in consistent form; i.e., all nodes within an element influence one another. An alternative formulation of this matrix can be obtained by lumping the off-diagonal terms onto the main diagonal and is known as the lumped formulation. In addition to these two formulations, we also implemented a lumped formulation in which the weights for off-diagonal terms are set to zero and the weights for diagonal terms are set to the fractional area of the element associated with the node (i.e., 1/3 for triangular and 1/4 for rectangular elements). This scheme is similar to a finite-difference approach and is consistent with a trapezoidal scheme generally accepted for computing the mass balance. This is the scheme we used in the examples presented later in the paper.

Equation (7) is solved by using a time-weighting scheme which results in the following equation

$$\left(\xi[A] + \frac{[B]}{\Delta t}\right)^{k+1/2}\{\psi\}^{k+1} = \left((\xi - 1)[A] + \frac{[B]}{\Delta t}\right)^{k+1/2}\{\psi\}^k + \{F\}^{k+1/2} - \{Q\}^{k+1/2} \qquad (9)$$

where the superscript denotes the time level; and ξ is the time-weighting factor and varies between zero (for explicit scheme) and one (for fully implicit scheme).

The set of algebraic equations are, then, solved using a preconditioned conjugate gradient-like method (Reid, 1971; Young, 1971). The incomplete LU decomposition of the coefficient matrix is used as a preconditioner to enhance the convergence properties of the method. Even with zero level of fill-in during the decomposition process, the convergence of conjugate gradient iteration was found to be adequate. Details of the procedure are given in Yeh and Srivastava (1990). Only the nonzero matrix elements need to be stored, thus saving a huge amount of computer memory as compared to the direct banded matrix solvers. Either a Picard or Newton iteration scheme is used to accomplish the convergence of the solution of the nonlinear algebraic equations. Automatic time stepping is used to ensure the convergence of the nonlinear iterations necessary due to the dependence of the coefficient matrices [equations (8)] on the pressure head. The convergence of iterations is checked by comparing the maximum head difference between two successive iterations with a prescribed tolerance. If the number of iterations exceeds a specified maximum or if the solution is

found to be diverging, the time step is reduced by a specified factor. On the other hand, if the convergence is very rapid, the time step is automatically increased.

To avoid the loss of one order of accuracy due to the numerical differentiation in approximating the specific discharge field, a finite-element type procedure (Segol, 1976; Yeh, 1981) was employed, in which the velocities are obtained from the computed head field by applying the Galerkin technique separately to the flux equation

$$q_i = -K_{ij} \frac{\partial}{\partial x_j} (\psi + \beta_g x_2) \tag{10}$$

Using the same type of shape functions, N_I, for the velocity components, (10) cay be written as

$$[A_q]\{q_i\}^{k+1} + [B_{qi}]^{k+1}\{\psi\}^{k+1} + \{C_{qi}\}^{k+1} = 0$$
$$\text{for } i = 1, 2 \tag{11}$$

in which:

$$A_{qIJ} = \Sigma_e \int_{A^e} N_I N_J \, dA \tag{12a}$$

$$B_{qiIJ} = \Sigma_e \int_{A^e} N_I (N_L K_{ij}^L) \frac{\partial N_J}{\partial x_j} \, dA \tag{12b}$$

$$C_{qiI} = \beta_g \Sigma_e \int_{A^e} N_I (N_L K_{i2}^L) \, dA \tag{12c}$$

Though this procedure involves solution of NN simultaneous equations for each velocity component, the coefficient matrix is time invariant and has to be inverted only once during the entire simulation.

Transport equations (2) are solved using one-step reverse particle tracking for the advective transport (called MMOC for modified method of characteristics) and the regular Galerkin FEM for the dispersive transport. In the MMOC, the partial time derivative in equation (2a) is converted to a total derivative along the characteristic lines by using

$$\frac{Dc}{Dt} = \frac{\partial c}{\partial t} + \frac{q_i}{\theta(1 + k_3)} \frac{\partial c}{\partial x_i} \tag{13}$$

The finite-difference form of the total derivative can be written as

$$\frac{Dc}{Dt} = \frac{c^{k+1} - c_n^{\,k}}{\Delta t} \tag{14}$$

in which $c_n^{\,k}$ is the concentration at the time level k at the corresponding spatial position along the characteristic line. After applying the Galerkin technique to the dispersive part of the equation, the concentration at a time step is given by

$$\left[\xi[A_c] + \left(\frac{\xi k_1}{1 + k_2 \xi \Delta t} + \frac{1 + k_3}{\Delta t}\right)[B_c]\right]^{k+1/2} \{c^{k+1}\} =$$

$$\left(-(1 - \xi)[A_c] - \frac{(1 - \xi) k_1}{1 + k_2 \xi \Delta t}[B_c]\right)^{k+1/2} \{c^k\} +$$

$$\frac{1 + k_3}{\Delta t}[B_c]^{k+1/2}\{c_n^{\,k}\} + \frac{[B_c^*]}{1 + k_2 \xi \Delta t}\{c_k^{*k}\} - \{Q_c\}^{k+1/2} \quad \ldots . (15)$$

in which:

$$A_{cIJ} = \Sigma_e \int_{A^e} D_{ij} \frac{\partial N_I}{\partial x_i} \frac{\partial N_J}{\partial x_j} \, dA \tag{16a}$$

$$B_{cIJ} = \Sigma_e \int_{A^e} \theta N_I N_J \, dA \tag{16b}$$

$$B^*_{cIJ} = \Sigma_e \int_{A^e} (1 - f) \rho_b k_2 N_I N_J \, dA \tag{16c}$$

$$Q_{cI} = \Sigma_e \left(\int_{A^e} N_I q_s (c - c_s) \, dA - \int_{B^e} N_I q_{cb} \, dB\right) \tag{16d}$$

The boundary integral in (16d) is performed over boundaries with the specified dispersive flux q_{cb}.

The location for the determination of $c_n^{\,k}$ is obtained by fourth-order Runge-Kutta integration of the equation:

$$\frac{dx_i}{dt} = \frac{q_i}{\theta(1 + k_3)} \tag{17}$$

resulting in the following expressions:

$$dx_i^{\,1} = -\frac{\Delta t (q_i^{\,k+1/2})_{x_i}}{(\theta^{k+1/2})_{x_i}(1 + k_3)} \tag{18a}$$

$$dx_i^{\,2} = -\frac{\Delta t (q_i^{\,k+1/2})_{x_i + dx_i^{\,1}/2}}{(\theta^{k+1/2})_{x_i + dx_i^{\,1}/2}(1 + k_3)} \tag{18b}$$

$$dx_i^{\,3} = -\frac{\Delta t (q_i^{\,k+1/2})_{x_i + dx_i^{\,2}/2}}{(\theta^{k+1/2})_{x_i + dx_i^{\,2}/2}(1 + k_3)} \tag{18c}$$

$$dx_i^{\,4} = -\frac{\Delta t (q_i^{\,k+1/2})_{x_i + dx_i^{\,3}}}{(\theta^{k+1/2})_{x_i + dx_i^{\,3}}(1 + k_3)} \tag{18d}$$

and

$$x_i^{\,k} = x_i + (1/6)(dx_i^{\,1} + 2dx_i^{\,2} + 2dx_i^{\,3} + dx_i^{\,4}) \tag{18e}$$

During the back-tracking algorithm, the particle concentration is determined by using linear shape functions and concentrations at the nodes of the element. If the particle crosses an inflow boundary, it is assigned the concentration at the boundary. At no-flow boundaries, the particle is reflected back into the domain. After solving for the liquid phase concentration from equation (15), the adsorbed phase concentration is obtained from

$$c_k^{*k+1} = \frac{[1 - k_2(1 - \xi)\Delta t]c_k^{*k} + \frac{(1 - \xi) k_1 \theta \Delta t}{\rho_b} c_k + \frac{\xi k_1 \theta \Delta t}{\rho_b} c_{k+1}}{1 + k_2 \xi \Delta t} \quad \ldots . (19a)$$

and

$$c_e^{*k+1} = \frac{k_3 \theta}{\rho_b} c^{k+1} \tag{19b}$$

If the time-weighting factor ξ is taken to be 0, we obtain an explicit scheme which, along with the lumping of the mass matrix, results in direct evaluation of nodal concentration at time level (k + 1) without solving a set of linear simultaneous equations.

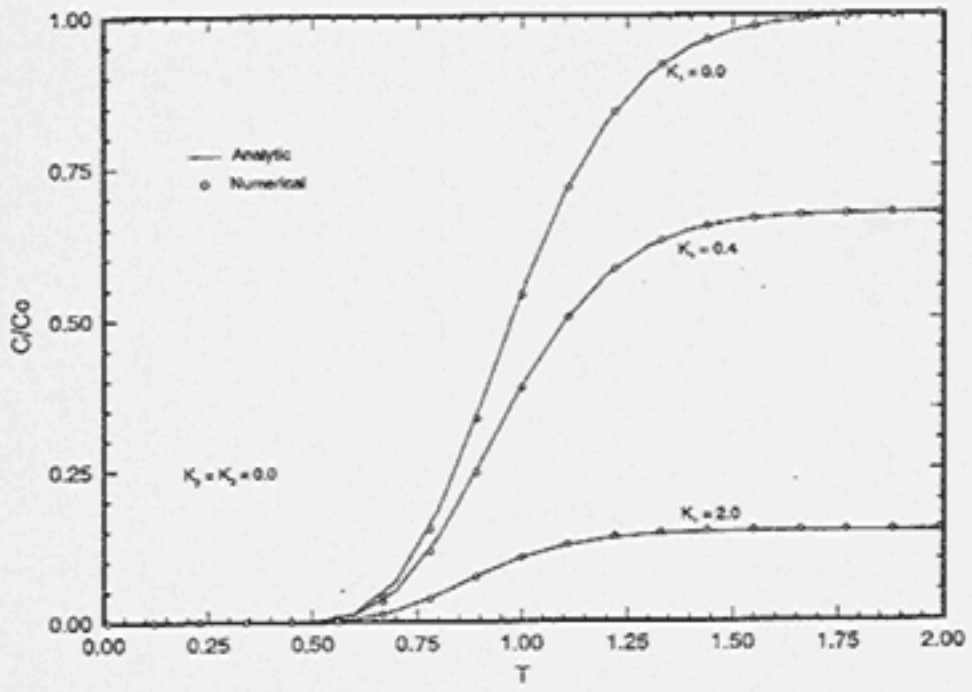

Fig. 1. Breakthrough curves for different values of K_1.

Applications

1-D Saturated Flow and Solute Transport

The numerical scheme described above is first used to simulate the transport of reactive chemicals in a soil column under saturated conditions. Cameron and Klute (1977) present an analytic solution to this problem assuming a prescribed concentration (c_0) boundary condition at the upstream end and zero concentration at infinity. The non-dimensional parameters used in this analysis are defined as

$$T = \frac{vt}{L} \qquad B = \frac{vL}{4D}$$

$$K_1 = \frac{Lk_1}{v} \qquad K_2 = \frac{Lk_2}{v} \qquad K_3 = k_3$$

where: t is time, L is the length of the column, v is the seepage velocity, D is the hydraulic dispersion coefficient, and B is the Brenner number.

The breakthrough curve (plots of dimensionless time versus dimensionless concentration, c/c_0, at the outlet) for $B = 10$, $K_2 = 0$, and $K_3 = 0$, and different values of K_1 are shown in Figure 1. The parameters used for the numerical simulations are: seepage velocity 1 cm/hr, column length 10 cm, longitudinal dispersivity 0.25 cm, mesh size 0.1 cm, and time step 0.1 hour. The mesh Peclet number is kept at 0.4, and the Courant number is equal to 1 to eliminate the interpolation errors. The time-weighting factor in this simulation is 1.0, resulting in the fully implicit scheme. As seen from this figure, the numerical results are in perfect agreement with the analytical solution. Figure 2 shows the longitudinal concentration profiles at different times for $K_1 = 2.0$. To observe the effect of the Courant number, simulations for $K_1 = 1.0$, $K_2 = 0.1$, and $K_3 = 4.0$ are performed for three different Courant numbers, 0.5, 1.0, and 1.5. Courant numbers different from 1.0 introduced no noticeable interpolation errors in the back-tracking calculations. The model is then applied to simulate the behavior of the chemical Atrazine, with $B = 20$, $K_1 = 0.48$, $K_2 = 0.18$, and $K_3 = 3.52$, in a soil column of Honeywood silt loam. Breakthrough data are reported by Elrick et al. (1966). The comparison of simulated versus observed data is shown in Figure 3. The parameters used for the numerical simulation are: seepage velocity 0.64 cm/hr, column length 15 cm, longitudinal dispersivity 0.1875 cm, saturated conductivity 0.3283 cm/hr, porosity 0.513, bulk density 1.42 gm/cm^3, forward rate constant 0.02048 per hr, backward rate constant 0.0768 per hr, and the equilibrium constant 3.52. The mesh size is kept at 0.1 cm and the time step is 0.7 hr. It is seen that the MMOC, using the parameters obtained by fitting the analytic solution to the observed data (Cameron and Klute, 1977), duplicates the observed breakthrough data very well.

2-D Solute Transport in a Steady Uniform Flow Field

The purpose of this application is to test the validity of the model for the case where both longitudinal and transverse dispersion exist. Bruch and Street (1967) developed an exact analytical solution for the advection-dispersion equation in a 2-D semi-infinite medium of finite width given a finite-line source. We compare the solution of MMOC with

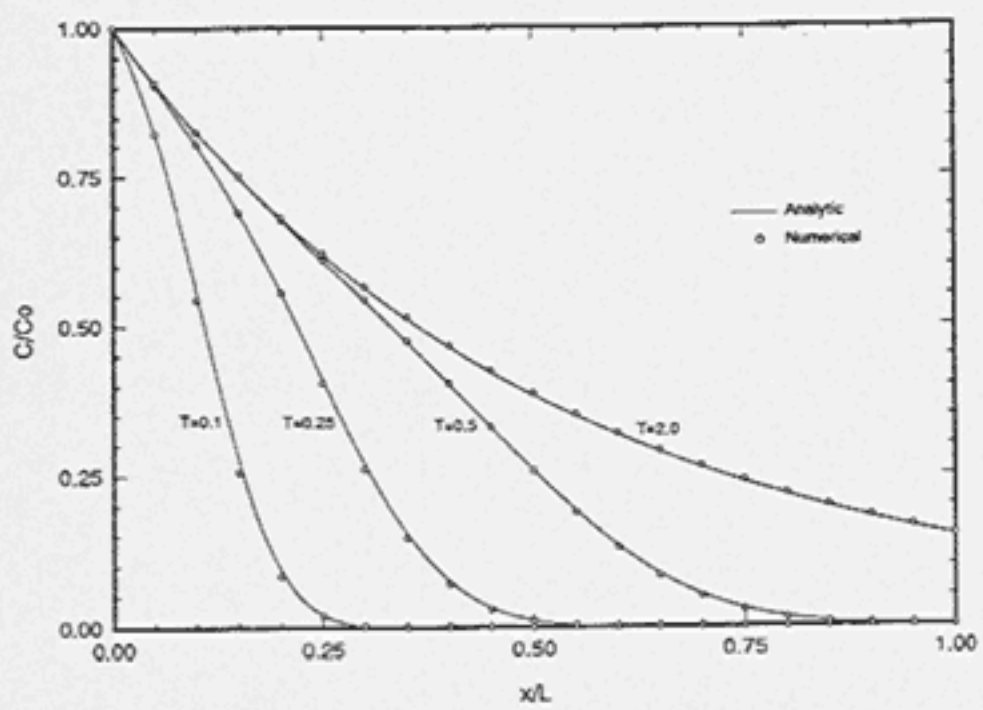

Fig. 2. Longitudinal concentration profiles at different times for $K_1 = 2$.

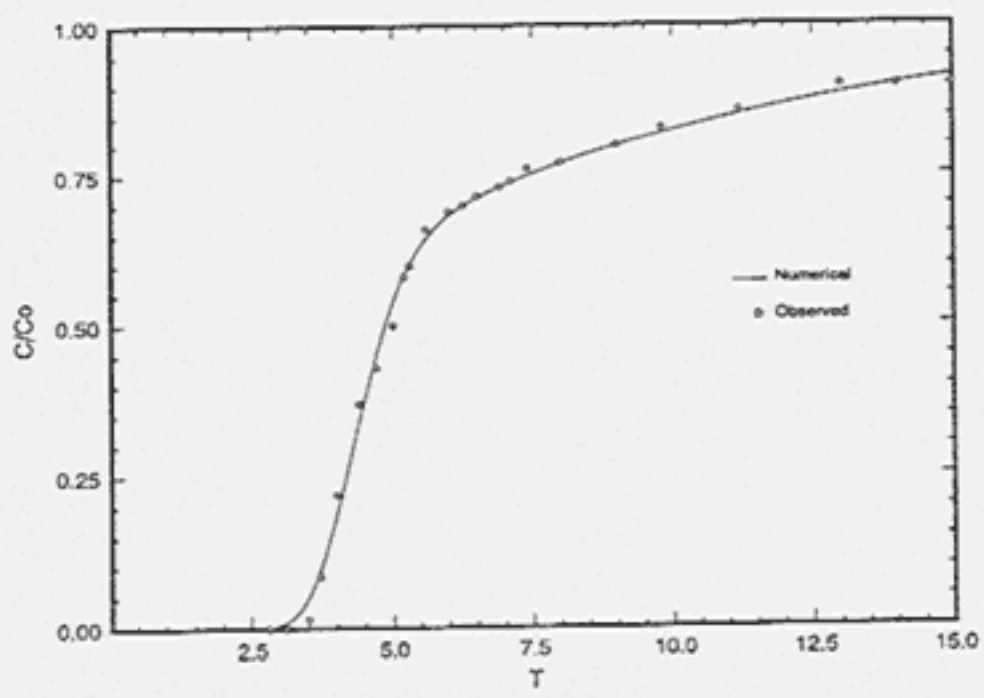

Fig. 3. Breakthrough curves for Atrazine in Honeywood silty loam column.

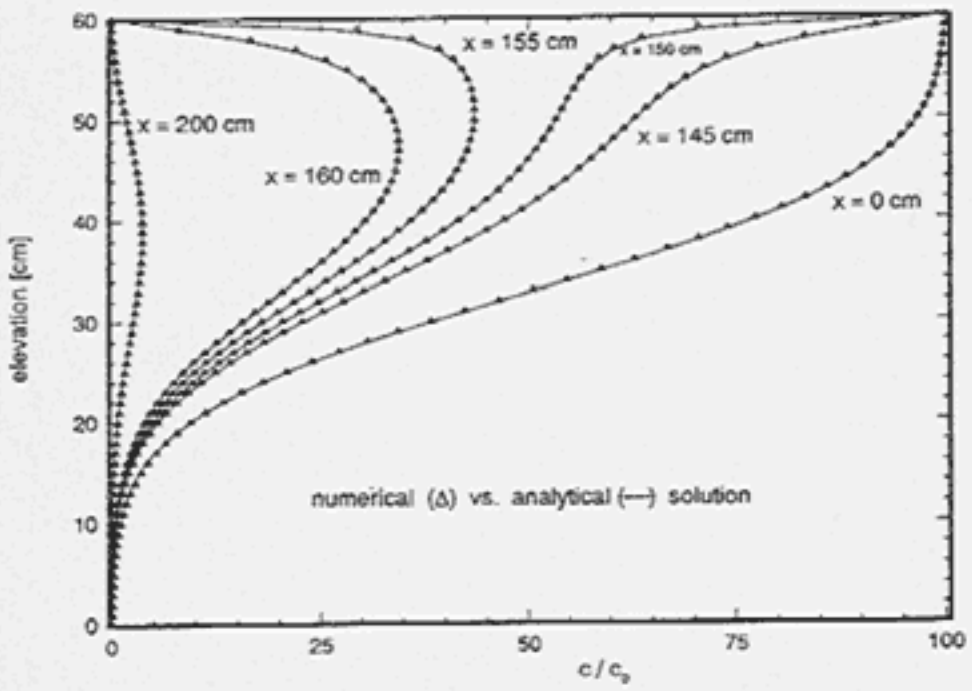

Fig. 4. Concentration distribution at various vertical sections.

the analytic solution for the hypothetical case of a vertical soil profile with a uniform flow field and the following boundary conditions:

$c/c_0 = 1$	$0\ \text{cm} \leq x \leq 152.5\ \text{cm}$, $z = 300\ \text{cm}$
$c/c_0 = 0$	$152.5\ \text{cm} < x \leq 300.0\ \text{cm}$, $z = 300\ \text{cm}$
$c/c_0 = 0$	$z = 0\ \text{cm}$
$\Delta c/\Delta x = 0$	$x = 0\ \text{cm}$, $x = 300\ \text{cm}$

The parameters to the transport equation are: longitudinal dispersivity $\alpha_L = 10$ cm, transverse dispersivity $\alpha_T = 5$ cm, velocity = 63.45 cm/day. Square finite elements of 5 cm width are specified (thus the Peclet number $Pe \leq 1$), and the time-step $\Delta t = 0.01$ days is chosen such that the Courant number $Co < 1$. As shown in Figure 4, the numerical solution is in excellent agreement with the analytical solution. The solute profiles practically coincide, and the differences between the two solutions are less than 1% anywhere in the domain.

2-D Saturated Flow and Transport from a River Towards a Well

To ascertain the accuracy of the particle tracking algorithm in a nonuniform flow field, horizontal two-dimensional flow and transport from a river towards a well is simulated. The velocity field and the location of concentration front starting from the river can be analytically obtained using a sharp interface (i.e., without considering dispersion) approach (Muskat, 1937). At any time, the concentration front obtained from the numerical simulations should then correspond to the location of particles at that time as given by the analytic solution. However, because of the highly nonuniform nature of the velocity field, the Courant number is very different from 1.0, thus introducing some interpolation error during back-tracking. This causes artificial (numerical) dispersion of the concentration front, and therefore the simulated front is dispersed about the mean position, even when the dispersivity is set to zero in the simulation. To compare the analytic and simulated results, the simulated concentration front is assumed to be located at a concentration equal to half of that in the river ($c/c_0 = 0.5$).

The numerical simulation is performed using a domain of 60 m × 40 m with the well being at a distance of 10 m from the river boundary. The analytical solution is for an infinite domain, but we truncate the river at 30 m on either side of the well to achieve a reasonable computational time without sacrificing much accuracy. The grid size is chosen as 0.2 m in both x and y directions, and a total of 60,000 elements with 60,401 nodes are obtained. The pumping rate at the well is kept at 5 m^3/hr and the time step is varied from 0.01 hr to 0.1 hr. Figure 5 shows the position of the concentration front at different times obtained from the numerical simulation and the corresponding analytic solution. As mentioned earlier, the numerical concentration front is the location of the 50% contour, and a narrow band around this line represents the complete numerical concentration distribution. This band is not shown in the figure but is about 2 m in thickness at $t = 40$ hours. A very good agreement between the model results and the theoretical values is obtained. Slight differences near the edges of the plot are thought to be an artifact of the numerical model resulting from truncating the infinite river boundary to 30 m on either side of the well and putting a no-flow boundary there.

1-D Transient Flow and Transport in Unsaturated Media

Few analytical solutions are available for flow and solute transport in unsaturated porous media. Wilson and Gelhar (1984) presented an approximate analytical solution to compute one-dimensional infiltration of solutes into unsaturated soils both under steady-state and transient flow conditions. We simulate their problem with our model based on a two-dimensional finite-element grid of 135 elements in the z direction and 10 elements in the x direction. The side length of the square elements is 1 cm.

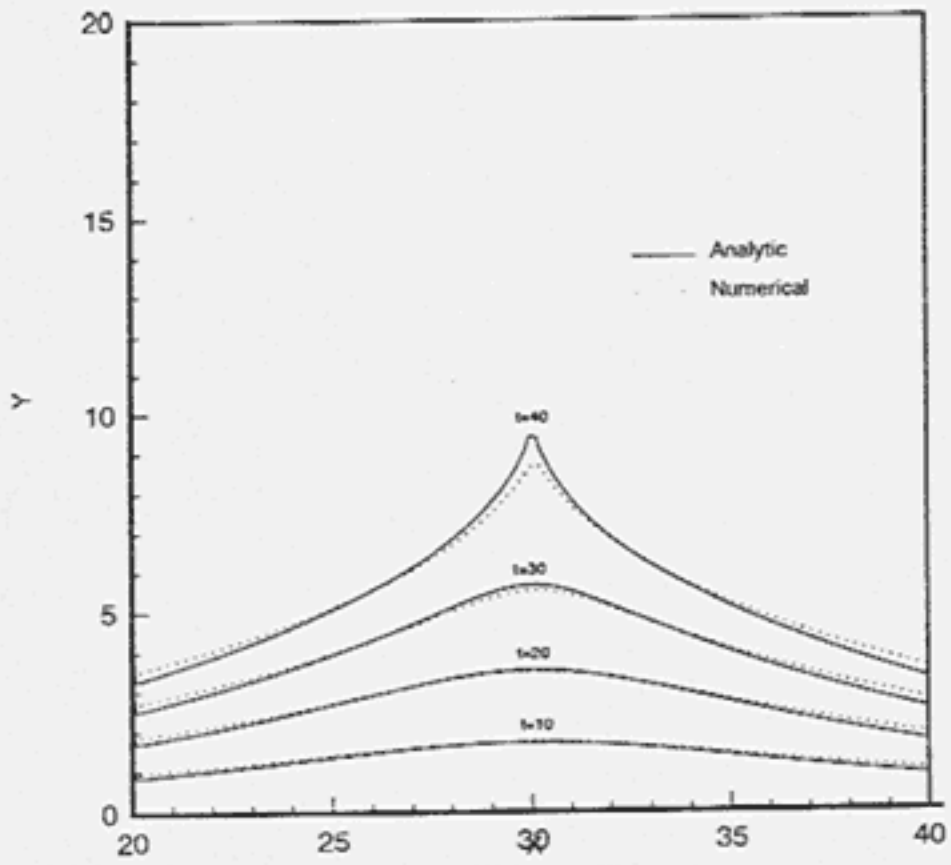

Fig. 5. Location of concentration front at different times.

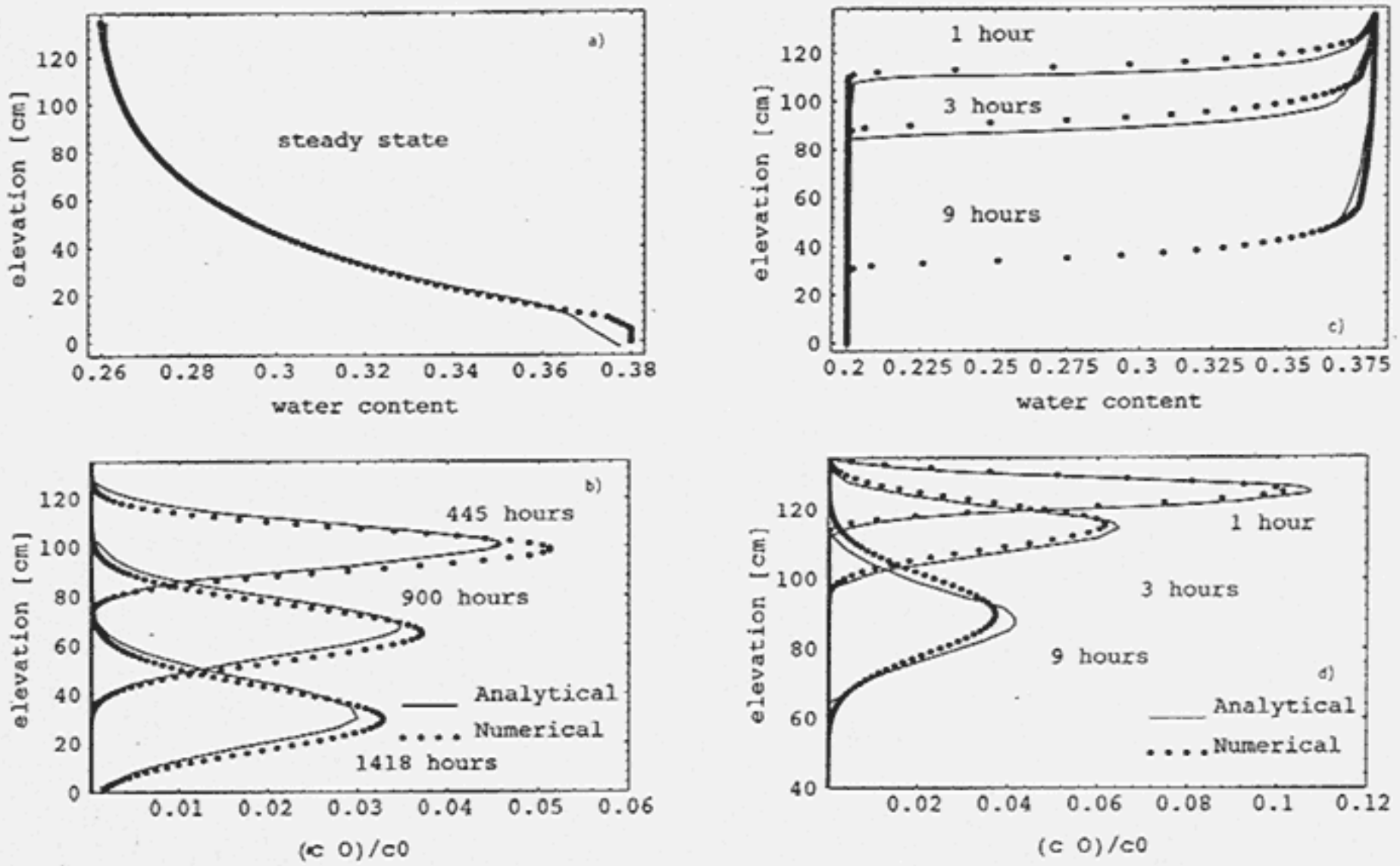

Fig. 6. (a) Soil moisture profile for steady-state infiltration. (b) Concentration profiles at different times under the steady-state infiltration. (c) Moisture profiles at various times under transient infiltration. Note that only partial moisture profile (analytical solution) at nine hours is presented in Wilson and Gelhar. (d) Concentration profiles at different times under the transient infiltration.

The flow problem in the analytical solution of Wilson and Gelhar is given by a water-content-based form of Richards' equation with θ_s (saturation) and θ_0 prescribed at bottom and top, respectively, of a soil column. The relationships for $\theta(\psi)$ and $K(\psi)$ used in this model, which solves the pressure-based form of Richards' equation, are equivalent to those for $\psi(\theta)$ and $K(\theta)$ given in Wilson and Gelhar:

$\theta_0 = 0.2$

$\theta_s = 0.38$

$\psi(\theta) = -1377 \exp(-10.5\,\theta) \qquad \theta \leq 0.37$

$\psi(\theta) = -1.8\text{E}+07 \exp(-35.8\,\theta) \qquad \theta > 0.37$

$K(\theta) = 1.944\text{E}-06 \exp(35.8\,\theta)$

$D(\theta) = 0.0281 \exp(25.3\,\theta) \qquad \theta < 0.36$

$D(\theta) = 259.0 + 9.91\text{E}+04(\theta - 0.36) \qquad 0.36 \leq \theta \leq 0.37$

$D(\theta) = 1250 \qquad \theta > 0.37$

However, a translation of these properties from $\psi(\theta)$, $K(\theta)$, and $D(\theta)$ to $\theta(\psi)$, $K(\psi)$, and $C(\psi)$ are required and involves some approximations. For the steady-state solution with our model, a pressure head of -17 cm is prescribed at the bottom of the soil column, and a constant flux of $q = 0.48$ cm/day is assigned as a boundary condition at the top of the column. The pressure head at the bottom of the column is chosen to best-fit the soil moisture profile obtained by our model with the soil moisture profile given in Wilson and Gelhar. In the transient flow problem presented below, the uniform initial head corresponding to the initial water content of $\theta_0 = 0.2$ in Wilson and Gelhar is used. At $t > 0$, a head equivalent to $\theta_s = 0.38$ is assigned to the top of the column, and a head equivalent to θ_0 is the boundary condition at the bottom of the column.

For the solute transport example, the background concentration of the solute is assumed zero. The boundary conditions to the solutions by Wilson and Gelhar are given as a unit solute pulse (pulse length equal to 1 cm) at the top of the soil column at $t = 0$ days, and zero concentration at infinite depth. In our numerical simulation, a constant non-zero concentration boundary condition is prescribed at the top for the time necessary to infiltrate 1 cm of water. Then the boundary is set to zero concentration. Molecular diffusion is neglected and the hydrodynamic dispersivity is set to 1.013 cm as in Wilson and Gelhar. The grid-Peclet number is $1/1.013 \approx 1$, and the Courant number is much less than 1 at any time ($\Delta t = 0.01$ days).

As shown in Figure 6a, the steady-state soil moisture profiles of the analytical and numerical solutions are identical with the exception of the conditions near the water table. Some discrepancies exist between the numerical and the analytical solution of the solute transport equation (Figure 6b). The numerical solution produces a higher peak concentration than the approximate analytical solution, and the plume resulting from the numerical model moves slightly faster than that from the analytical solution, but the spreadings of the solute pulse are nearly identical. The numerical solution exhibits a mass surplus of 4% at all times after the injection, a condition that can be adjusted by slightly decreasing the initial solute application time.

Comparison of numerical and analytical moisture and

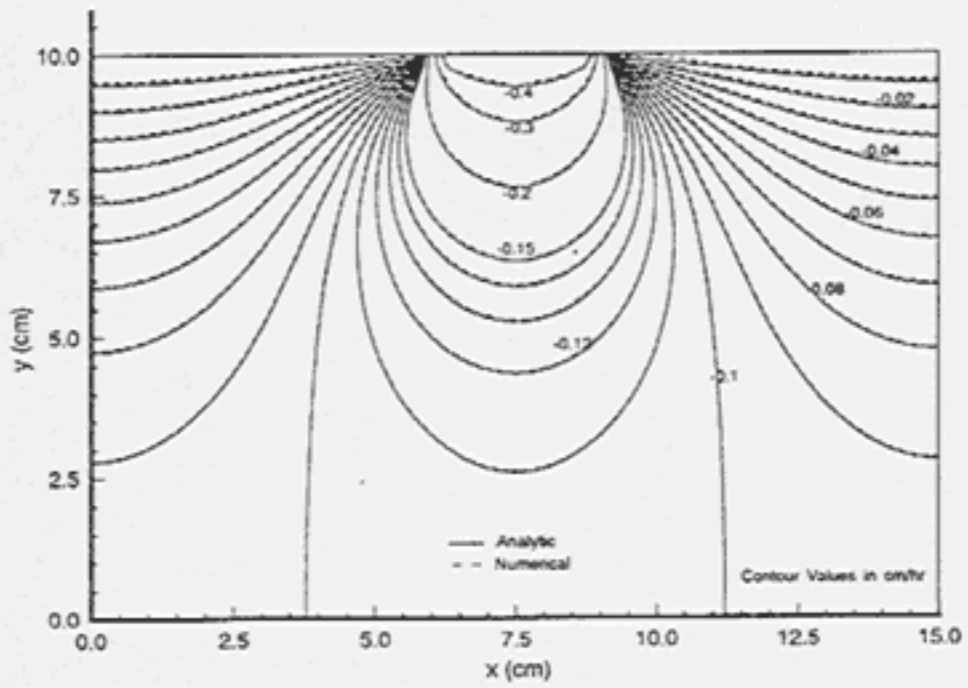

Fig. 7. Contours of the vertical component of specific discharge.

concentration profiles for the transient case are presented in Figures 6c and 6d. As illustrated in Figure 6c, the wetting profiles calculated by our model lag behind the analytical ones. As a result, the solute plumes derived from the analytical solution are slightly ahead of the ones from our model. The mass balance errors in these cases are less than 0.5%. These discrepancies can probably be attributed to the fact that the analytical solution is an approximation and that soil unsaturated properties used in our model are not exactly identical to those used by Wilson and Gelhar. However, the results are, in general, satisfactory.

2-D Steady Flow and Transient Transport in Unsaturated Media

To test our model for a more complex flow field, the model is applied to simulate solute transport in a hypothetical soil profile under steady flow toward the water table from a strip source where the analytical solution for the flow can be derived. In our simulation, steady-state flow and velocity fields are obtained and then a constant concentration boundary condition is imposed on the strip source to simulate the transport of solute under the unsaturated conditions. Exponential relationships are assumed between pressure and conductivity, and pressure and moisture content of the hypothetical soil [Appendix, equation (A1)]. The soil hydraulic parameters used are: $K_s = 1$ cm/hr, $\alpha = 0.01$/cm, $\theta_s = 0.44$, $\theta_r = 0.067$, $\alpha_L = \alpha_T = 0.0$ cm, $D_0 = 0.0$ cm^2/hr, and the initial conditions are assumed to be hydrostatic.

The domain is divided into 2500 elements with 2601 nodes with $\Delta x = 0.3$ cm and $\Delta z = 0.2$ cm. The time-step length is changed from an initial value of 0.1 hr to a maximum of 0.2 hr, and 55 time steps are required to simulate the solute distribution to 10 hours. The CPU time required for this problem is 209 seconds on an IBM RISC 6000/550 workstation, out of which about half is for the steady-state flow solution. Exact analytical solutions for the velocity components in x and z directions are derived (Appendix A) to check the accuracy of the numerical solution. Figure 7 shows the contours of the vertical velocity component from the analytic results, for the steady-state solution, and from the numerical calculation. Clearly, the numerical results are in excellent agreement with the analytic solutions. A similar agreement is obtained for the horizontal velocity component. This indicates that, for this problem, the inconsistency of assuming both the head and the velocity components as linear in equation (10) does not adversely affect the numerical results. In addition, these results confirm the explanation for the discrepancies between the numerical model and the approximate analytical solutions given in the previous one-dimensional flow case.

Simulated solute distribution, resulting from pure convection, at 10 hours, is depicted in Figure 8. The simulated distribution appears reasonable and there is no numerical oscillation. However, numerical dispersion of about 0.5 cm in either side of the front is observed. Unfortunately, no analytic solutions for solute transport for the specified flow field are available and thus, we cannot verify the accuracy of the simulated results. Our results show that the MMOC calculations produce a mass balance error of less than 5%.

Simulation of Moisture Movement in a Sandbox

To further test the ability of our model, the model is used to simulate the moisture movement from a point source through alternating layers of medium and coarse sand in a laboratory sandbox (Mathieu, 1988). The unsaturated hydraulic properties of the materials are represented by the van Genuchten model. That is, the moisture content-suction relationship (water release curve) of the materials is given by

$$\theta(\psi) = (\theta_s - \theta_r)\,[1 + (\alpha\psi)^n]^{-m} + \theta_r \qquad (20)$$

Then the hydraulic conductivity-suction relationship is described by

$$K(\psi) = K_s \frac{(1 - (\alpha\psi)^{n-1}\,[1 + (\alpha\psi)^n]^{-m})^2}{[1 + (\alpha\psi)^n]^{m/2}} \qquad (21)$$

where K_s is the saturated hydraulic conductivity, and ψ is the suction. θ_s and θ_r are moisture content at saturation, and residual moisture content, respectively. α and n are parameters controlling the curvature of the relationships and $m = 1 - 1/n$. The parameters for the two sands are: $K_s = 3.26$ m/hr, $\theta_s = 0.44$, $\theta_r = 0.067$, $\alpha = 9.13$ m^{-1}, and $n = 4.27$ for the medium sand; and $K_s = 4.05$ m/hr, $\theta_s = 0.446$, $\theta_r = 0.047$, $\alpha = 14.6$ m^{-1}, and $n = 10.16$ for the coarse sand (Yeh and Harvey, 1990). A uniform pressure head of -10 m is used as the initial conditions for both the experiment and the numerical model, and a flux of 1.62 m/hr is applied near the top corner. The sandbox, 150 cm wide and 16 cm deep, is discretized into 4832 elements with 5033 nodes with mesh size varying from 0.5 cm to 1.0 cm. The time-step size is changed from an initial value of 0.001 hr to a maximum value of 0.05 hr. Figures 9a and b show the simulated moisture distribution and a photograph of the observed wetting front. Although no measurements of moisture content or soil water tension are available for a quantitative comparison, an excellent qualitative agreement is clearly seen. This resemblance demonstrates that the finite-element models are capable of representing sharp material interfaces. This can be attributed to the fact that the

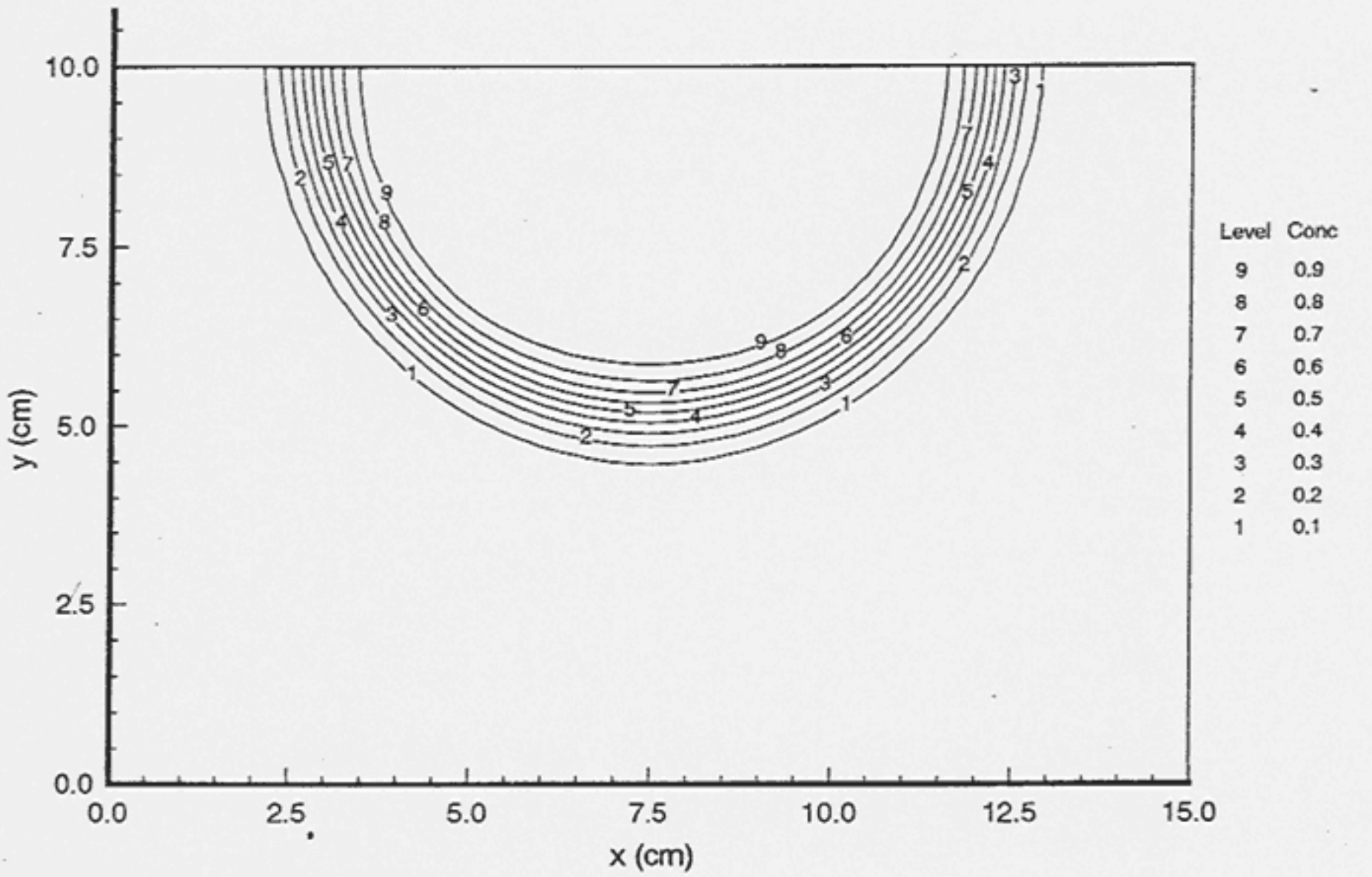

Fig. 8. Simulated concentration distribution at 10 hours.

interfacial boundary conditions are incorporated during the assemblage of the element matrices. Finite-difference models, on the other hand, tend to smooth the front near these interfaces. In addition, this comparison confirms the ability of our model to tackle highly nonlinear unsaturated flow under very dry conditions.

Summary and Discussion

A two-dimensional finite-element model for the simulation of the transport of a chemically reactive solute is developed by combining the recent developments in the fields of numerical methods and chemical reaction of solvents. The accuracy of this model is tested against analytic solutions and observed values for both saturated and unsaturated flow and transport problems. Some observations based upon the various simulation runs with our model are summarized below: (1) The adaptive time stepping and lumped scheme ensure convergence of the solution to the unsaturated flow problem. Small time-step sizes will speed up the convergence at each time step. This is due to the fact that under these conditions, the coefficient matrix becomes diagonally dominant and radius of convergence is greatly expanded (Fletcher, 1988). The trade-off, however, is that it will take a large number of time steps to finish the simulation resulting in a possible increase in interpolation error during reverse particle tracking. Large grid sizes have a similar effect on the convergence of the solution but the discretization error will increase. (2) A fully explicit scheme can be used in conjunction with the MMOC to save computer time and storage space without limiting the time step to a very small value. (3) In most flow situations the application of the Galerkin scheme to the flux equation results in a quite accurate velocity field despite the assumption of linear variation of velocity being inconsistent with a linear head variation. Although the mixed finite-element approach (e.g., Chiang et al., 1989) may provide a more accurate velocity solution, the fact that it results in large and poorly conditioned matrices for heterogeneous aquifers (Allen et al., 1992) makes the Galerkin scheme applied to the flux equation more favorable. Finally, the MMOC approach alleviates the numerical oscillation problem in convection-dominated solute transport that commonly exists in a finite-element solute transport model, but it suffers from numerical dispersion as do other numerical models. A higher order shape function for the interpolation can reduce this problem but may introduce numerical oscillations (Cheng et al., 1984).

The FORTRAN source code of the model is available through the first author at the Department of Hydrology and Water Resources, University of Arizona, Tucson, AZ 85721 (phone: 602-621-5943).

Acknowledgments

This study is funded by EPA grant R-813899-01-1. We wish to thank the anonymous reviewers whose comments contributed to a better presentation of this article.

Appendix

The analytic solution of two-dimensional steady-state flow towards the water table is given below. The flow domain is of height H and length L, and the recharging strip extends from a distance a to b from the left-hand side. Both

the vertical sides are impervious, and the lower boundary is the water table. The flow through the strip is q. The origin of coordinates in the following expressions is at the lower left corner of the domain. The actual variables are denoted with an asterisk to distinguish them from the dimensionless forms. Exponential relations are assumed as follows:

$$K_x^* = K_{sx}\, e^{\alpha\psi} \quad K_z^* = K_{sz}\, e^{\alpha\psi} \quad \theta = \theta_r + (\theta_s - \theta_r)\, e^{\alpha\psi} \qquad \ldots . \text{(A1)}$$

where K_i^* is the hydraulic conductivity in the i direction.

Dimensionless variables are defined as

$$x = \alpha x^* \sqrt{K_{sz}/K_{sx}} \quad \text{so that } L = \alpha L^* \sqrt{K_{sz}/K_{sx}};$$

$$a = \alpha a^* \sqrt{K_{sz}/K_{sx}}; \quad b = \alpha b^* \sqrt{K_{sz}/K_{sx}} \qquad \text{(A2)}$$

$$z = \alpha z^* \quad \text{so that} \quad H = \alpha H^* \qquad \text{(A3)}$$

$$K = \frac{K_x^*}{K_{sx}} = \frac{K_z^*}{K_{sz}} \qquad \text{(A4)}$$

$$q = \frac{q^*}{K_{sz}} \qquad \text{(A5)}$$

The steady-state solution is then obtained as

$$K = e^{-z} + \frac{q(b-a)}{L}(1 - e^{-z}) + \frac{2q}{L}\, e^{(H-1)/2} \sum_{n=1}^{\infty} \frac{\{\sin(\lambda_n b) - \sin(\lambda_n a)\sinh(p_n z)}{\lambda_n\{\tfrac{1}{2}\sinh(p_n H) + p_n \cosh(p_n H)\}} \qquad \text{(A6)}$$

where $\lambda_n = (n\pi)/L$; and $p_n = \sqrt{\tfrac{1}{4} + \lambda_n^2}$.

The dimensionless Darcy velocity components in x and z directions are obtained as

$$V_x = \frac{V_x^*}{\sqrt{K_{sx} K_{sz}}} = -\frac{\partial K}{\partial x} \qquad \text{(A7)}$$

and

$$V_z = \frac{V_z^*}{K_{sz}} = -\left(\frac{\partial K}{\partial z} + K\right) \qquad \text{(A8)}$$

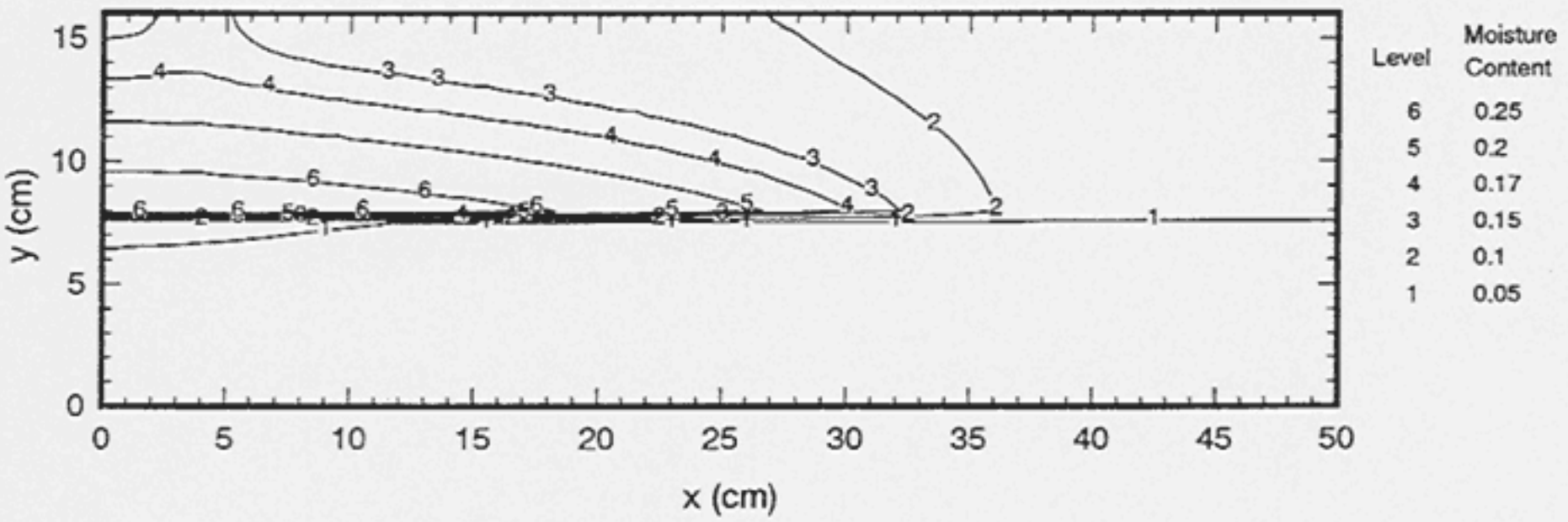

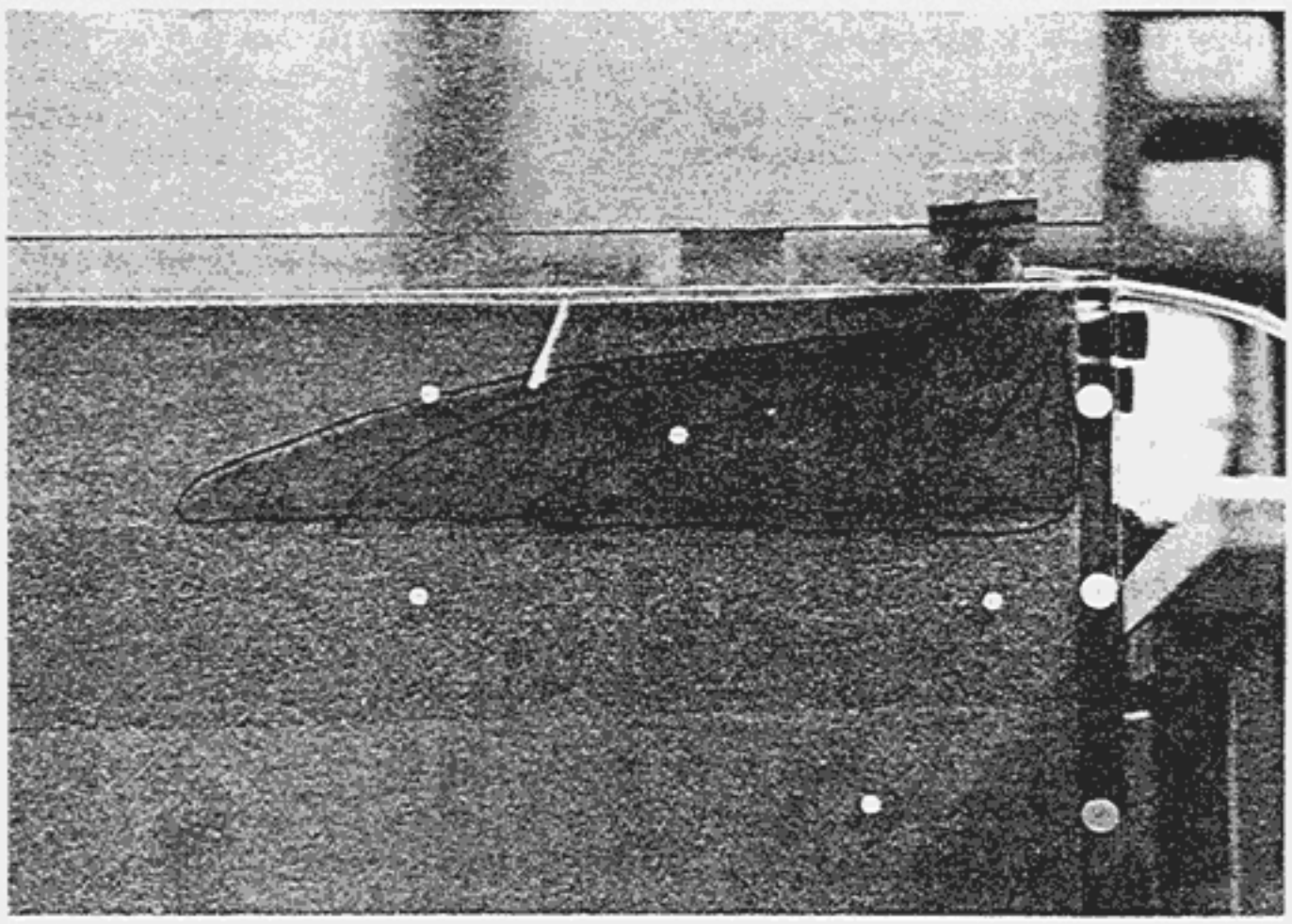

Fig. 9. Moisture content distribution at a given time in a sandbox: (a) numerical results; and (b) observed moisture distribution.

References

Allen, M. B., R. E. Ewing, and P. Lu. 1992. Well conditioned iterative schemes for mixed finite-element models of porous media flow. SIAM J. Sci. Stat. Comput. (To appear.)

Anderson, M. P. 1979. Using models to simulate the movement of contaminants through ground water flow systems. CRC Crit. Rev. Environ. Control. v. 9, pp. 97-156.

Bear, J. 1979. Hydraulics of Groundwater. McGraw Hill, New York.

Bruch, J. C. and R. L. Street. 1967. Two-dimensional dispersion. J. of the Sanitary Engineering Division, ASCE. v. 93, no. SA6, pp. 17-39.

Cady, R. 1991. An adaptive multi-dimensional finite element method for simulating advection-dispersion. Ph.D. dissertation, Dept. of Hydrology and Water Resources, Univ. of Arizona, Tucson, AZ.

Cameron, D. R. and A. Klute. 1977. Convective-dispersive solute transport with a combined equilibrium and kinetic model. Water Resour. Res. v. 13, no. 1, pp. 183-188.

Celia, M. A., E. T. Bouloutas, and R. L. Zarba. 1990. A general mass-conservative numerical solution for the unsaturated flow equation. Water Resour. Res. v. 26, no. 7, pp. 1483-1496.

Cheng, R. T., V. Casulli, and S. N. Milford. 1984. Eulerian-Lagrangian solution of the convection-dispersion equation in natural coordinates. Water Resour. Res. v. 20, no. 7, pp. 944-952.

Chiang, C. Y., M. F. Wheeler, and P. B. Bedient. 1989. A modified method of characteristics technique and mixed finite elements method for simulation of ground water solute transport. Water Resour. Res. v. 25, no. 7, pp. 1541-1549.

Coats, K. H. and B. D. Smith. 1964. Dead end pore volume and dispersion in porous media. Soc. Pet. Eng. J. v. 4, pp. 73-84.

Daus, A. D., E. O. Frind, and E. A. Sudicky. 1985. Comparative error analysis in finite element formulation of advection-dispersion equation. Adv. Water Resources. v. 8, pp. 86-96.

Deans, H. A. 1963. A mathematical model for dispersion in the direction of flow in porous media. Soc. Pet. Eng. J. v. 3, pp. 49-52.

Elrick, D. E., K. T. Erh, and H. K. Krupp. 1966. Applicaiton of miscible displacement techniques to soils. Water Resour. Res. v. 2, no. 4, pp. 717-727.

Fletcher, C.A.J. 1988. Computational Techniques for Fluid Dynamics, Springer Series in Computational Physics. Springer-Verlag, New York.

Goode, D. J. 1990. Particle velocity interpolation in block-centered finite difference groundwater flow models. Water Resour. Res. v. 26, no. 5, pp. 925-940.

Huyakorn, P. S. and K. Nilkuha. 1979. Solution of transient transport equation using an upstream finite element scheme. Appl. Math. Model. v. 3, pp. 7-17.

Konikow, L. F. and J. D. Bredehoeft. 1978. Computer model of two-dimensional solute transport and dispersion in ground water. In: Techniques of Water Resources Investigations, Book H, Ch. 2, U.S. Geol. Survey, Reston, VA.

Krupp, H. K., J. W. Biggar, and D. R. Nielsen. 1972. Relative flow rates of salt and water in soil. Soil Sci. Soc. Am. J. v. 36, no. 3, pp. 412-417.

Lassey, K. R. 1988. Unidimensional solute transport incorporating equilibrium and rate-limited isotherms with first order loss. 1. Model conceptualizations and analytic solutions. Water Resour. Res. v. 24, no. 3, pp. 343-350.

Lindstrom, F. T. and L. Boersma. 1973. A theory on the mass transport of previously distributed chemicals in a water-saturated sorbing porous medium, III. Exact solutions for first order kinetic sorption. Soil Sci. v. 115, no. 1, pp. 5-10.

Mathieu, J. T. 1988. Two-dimensional water flow through stratified unsaturated porous media: Laboratory sand-box experiments. M.S. thesis, Univ. of Arizona, Tucson, AZ.

Muskat, M. 1937. The Flow of Homogeneous Fluids Through Porous Media, McGraw-Hill, New York.

Neuman, S. P. 1984. Adaptive Eulerian-Lagrangian finite element method for advection-dispersion. Int. J. Numer. Methods Eng. v. 20, pp. 321-337.

Nkedi-Kizza, P., J. W. Biggar, H. M. Selim, M. Th. van Genuchten, P. J. Wierenga, J. M. Davidson, and D. R. Nielsen. 1984. On the equivalence of two conceptual models for describing ion-exchange during transport through an aggregated oxisol. Water Resour. Res. v. 20, no. 8, pp. 1123-1130.

Reid, J. K. 1971. On the method of conjugate gradients for the solution of large sparse systems of linear equations. In: Proc. Conf. on Large Sparse Sets of Linear Equations. Academic Press, New York.

Rubin, J. 1983. Transport of reactive solutes in porous media: Relation between mathematical nature of problem formulation and chemical nature of reactions. Water Resour. Res. v. 19, no. 5, pp. 1231-1252.

Segol, G. 1976. A three-dimensional Galerkin finite element model for the analysis of contaminant transport in variably saturated-unsaturated porous media. Dept. of Earth Sciences, Univ. of Waterloo, Waterloo, Canada.

Selim, H. M., J. M. Davidson, and R. S. Mansell. 1976. Evaluation of a two-site adsorption-desorption model for describing solute transport in soils. Proceedings, Summer Comp. Simul. Conf. pp. 444-448.

Sudicky, E. A. 1989. The Laplace transformation Galerkin technique: A time continuous finite element theory and application to mass transport in ground water. Water Resour. Res. v. 25, no. 8, pp. 1833-1846.

van Genuchten, M. Th. and P. J. Wierenga. 1976. Mass transfer studies in sorbing porous media, 1. Analytical solutions. Soil Sci. Soc. Am. J. v. 40, pp. 473-480.

Wilson, J. and L. W. Gelhar. 1981. Analysis of longitudinal dispersion in unsaturated flow, 1. The analytical method. Water Resour. Res. v. 17, no. 1, pp. 122-130.

Yanosik, J. and T. McCracken. 1979. A nine-point finite difference reservoir simulation for realistic prediction of adverse mobility ratio displacements. Soc. Pet. Eng. J. v. 19, pp. 253-262.

Yeh, G. T. 1990. A Lagrangian-Eulerian method with zoomable hidden fine-mesh approach to solving advection-dispersion equations. Water Resour. Res. v. 26, no. 6, pp. 1133-1144.

Yeh, G. T. 1981. On the computation of Darcian velocity and mass balance in the finite element modeling of groundwater flow. Water Resour. Res. v. 17, no. 5, pp. 1529-1534.

Yeh, T.-C. J. and R. Srivastava. 1990. Variably saturated flow and transport in 2 dimensions. Univ. of Arizona, Technical Report No. HWR 90-010.

Yeh, T.-C. J. and D. J. Harvey. 1990. Effective unsaturated hydraulic conductivity of layered sands. Water Resour. Res. v. 26, no. 6, pp. 1271-1279.

Young, D. M. 1971. Iterative Solution of Large Linear Systems. Academic Press, New York.